STM JOURNALS

Journal of
Automobile Engineering
and Applications

ISSN: 2455-3360
Volume 12, Issue 1, 2025
January–April
DOI Journal: 10.37591/JoAEA

https://journals.stmjournals.com/joaea

Research JoAEA

Hybrid Supercapacitor-Lithium Battery Performance for Electric Vehicles Under WLTP Protocol

C. Armenta-Déu[1,*], Erick Espín[2]

Abstract

This work aims to characterize the hybrid electric vehicle performance powered by a hybrid lithium battery/supercapacitor system. The characterization process runs on a standard driving cycle, the World Harmonized Light-duty Vehicle Test Procedure (WLTP), applied in many countries like the European Union but it can be applied to other standards like the American FTP-75 and the Japanese JC08 with similar operational results. The paper shows a combination between a lithium battery and a supercapacitor, improving the power source response towards the electric vehicle energy request and power demand, and increasing energy management and efficiency. The hybridization also contributes to lowering premature battery degradation and aging. The hybrid lithium battery/supercapacitor system performance analysis shows a higher reliability in power source operation and less battery wear due to the dual power source efficient management, and its appropriate application to the specific power range request. The main contribution of this work to the current state of the art is the absolute novelty of the method since the proposed procedure has never been applied before, despite commercial electric vehicles with lithium batteries and supercapacitor hybrid power sources being in production. This work represents a significant advance in the automotive industry since it provides car manufacturers and traffic policymakers with a practical tool to evaluate the performance of this type of vehicle under similar driving conditions to conventional EVs, thus allowing a more accurate and reliable comparative analysis. On the other hand, the paper proves the feasibility of the hybrid system and guarantees a continuous vehicle operation for specific driving conditions, providing a practical tool for electric vehicle manufacturers and designers. Additionally, the performance analysis of the hybrid lithium battery and supercapacitor system indicates that this configuration is also valid for storage unit used as power sources in applications other than electric vehicles, representing an added value for energy planners and designers.

Keywords: Electric vehicle (EV), supercapacitor, lithium battery, efficiency, driving cycle, performance evaluation

INTRODUCTION

Vehicle fleet electrification is a must [1-2] if we try to reduce the uncontrolled increase of greenhouse gasses (GHG) emissions [3-4], responsible for the global warming and climatic change in our planet [5-6]. Electric vehicles, however, confront resistance from potential drivers due to the lower driving range [7-8] and the need to change driving patterns [9-11]. Modern protocols arise to unify the electric vehicle driving range under specific driving conditions [12-15]. Among them, the most popular is the WLTP, implemented by all UNECE members [16]. This protocol applies to battery electric vehicles (BEVs); however, it is not valid for fuel cell electric vehicles (FCEV) or hybrid battery/fuel cell, battery / supercapacitor, fuel cell / supercapacitor, and any

***Author for Correspondence**
C. Armenta-Déu
E-mail: cardeu@fis.ucm.es

[1-2]Professor, Facultad de Ciencias Físicas. Universidad Complutense de Madrid. 28040 Madrid (Spain)

Received Date: March 20, 2025
Accepted Date: April 20, 2025
Published Date: April 29, 2025

Citation: C. Armenta-Déu[1], Erick Espín. Hybrid Supercapacitor-Lithium Battery Performance for Electric Vehicles Under WLTP Protocol. Journal of Automobile Engineering and Applications. 2025; 12(1): 41–

other hybrid combination. Recent works have studied the hybridization of batteries, fuel cells, and supercapacitors to characterize the performance of hybrid power sources in electric vehicles [17-20] or to determine the driving range [21-24]. These latter studies, however, are developed based on an existing protocol, currently but not necessarily WLTP, which generates deviations from the current driving range due to the different performance of batteries and hybrid power systems [25]. The main consequence of applying standard driving protocols developed for battery electric vehicles to hybrid power source electric vehicles is an inaccurate estimation of the driving range; therefore, specific protocols adapted to the power source configuration are mandatory.

This work analyzes the performance of an electric vehicle with a hybrid battery and fuel cell power source submitted to the WLTP protocol; the paper evaluates the driving range accurately considering the specific characteristics of the hybrid power source and the response to WLTP driving conditions. Since the hybrid power source reacts differently to the WLTP-specific changes in vehicle speed with time, the evolution of the battery and fuel cell performance represents an accurate approach to the adapted protocol.

OPERATIONAL BACKGROUND

Electric vehicle driving range results from the specific protocol application to a selected vehicle model. The protocol follows a defined pattern that tries to reproduce current driving conditions. This pattern consists of a series of route segments with specific setup acceleration, vehicle speed, and time for every segment. After applying this pattern, the protocol supplies the traveled distance for the cycle running time, corresponding to the specific battery Depth of Discharge (DOD). Extending the process until the battery is exhausted (DOD=1), the protocol delivers the electric vehicle driving range as the traveled distance in a cycle times the number of cycle repetitions.

The integration of energy storage systems, such as lithium batteries and supercapacitors, has gained interest due to their ability to improve efficiency and reliability in many applications. The lithium battery/supercapacitor combination offers a promising solution regarding power density, energy capacity, and peak current management [26].

Supercapacitors play a crucial role in managing peak power demands in hybrid systems due to their high power density and ability to charge and discharge quickly and efficiently. By harnessing electrostatic storage capacity, supercapacitors can instantly provide power to meet transient current demands, acting as fast-response energy storage in the system [27].

The designed hybrid power source consists of a supercapacitor coupled to a lithium battery; since any of the individual power sources may deliver energy to propel the vehicle, it is necessary to establish a protocol to determine which source supplies the energy at every moment. This protocol is based on power source characteristics; therefore, the supercapacitor powers the vehicle in acceleration or high power demand periods and the battery for other driving conditions. This configuration is because the supercapacitor can supply power at a higher discharge rate than the battery without degradation.

THEORETICAL FOUNDATIONS

The WLTP protocol follows the laws of Dynamics, where vehicle propelling force includes the contribution of inertial, drag, rolling, and weight components. Mathematically:

$$F = ma + \kappa v^2 + \mu mg + mg \sin \alpha \tag{1}$$

m, *a*, and *v* represent the vehicle mass, acceleration, and speed, κ and μ are the drag and rolling force coefficients, and α is the road slope. The drag coefficient depends on the vehicle's aerodynamic coefficient as in:

$$\kappa = (1/2)\rho C_x A \tag{2}$$

C_x and A are the vehicle aerodynamic coefficient and front area, and ρ is the air density.

The required power to propel the vehicle under specific driving conditions depends on the global force and average speed <v>, as:

$$P_d = F < v > \tag{3}$$

Since the route segments in the WLTP protocol are of short time and distance, we can determine average vehicle speed from the kinematic expression:

$$< v > = \frac{v_{end} + v_{init}}{2} \tag{4}$$

Analogously, the acceleration derives from the following equation:

$$a = \frac{v_{end} - v_{init}}{t_{op}} \tag{5}$$

Sub-indexes *init* and *end* account for initial and ending time of the process, and t_{op} corresponds to the time interval.

Therefore, to reproduce any WLTP protocol segment, we apply the specific driving conditions, speed, acceleration, and time; the energy consumption for this process derives from the expression:

$$\xi = \left[ma + (1/2)\rho C_x A v^2 + \mu mg + mg \sin\alpha \right] < v > t_{op} \tag{6}$$

The product $<v>t_{op}$ represents the traveled distance; replacing in equation 6:

$$\xi = \left[ma + (1/2)\rho C_x A v^2 + \mu mg + mg \sin\alpha \right] d \tag{7}$$

Equation 7 provides the energy consumption for a segment. Extending the process for the whole cycle:

$$\xi = \sum_{i=1}^{n} \left[\left(ma_i + \frac{1}{2}\rho C_x A v_i^2 + \mu_i mg + mg \sin\alpha_i \right) d_i \right] \tag{8}$$

Because this energy supplies current and voltage to the electric motor:

$$\sum_{i=1}^{n} \left[\left(ma_i + \frac{1}{2}\rho C_x A v_i^2 + \mu_i mg + mg \sin\alpha_i \right) d_i - \frac{V_{op} I_i}{\eta_g \eta_t} \right] = 0 \tag{9}$$

V_{op} is the operational voltage that matches the electric motor, battery, and supercapacitor output voltage. Since the electric motor must operate at constant voltage, V_{op} remains unchanged for the whole process. I_i is the discharge current, which varies according to the power demand, and η_g and η_t are the power generation and energy transmission efficiency.

The energy supplied by the battery generates a discharge computed by the DOD coefficient, expressed as:

$$DOD_i^{bat} = \frac{\xi_i}{V_{op} C_i^{bat}} = \frac{\eta_g V_{op} I_i t_i}{V_{op} C_i^{bat}} = \frac{\eta_g I_i t_i}{C_i^{bat}} \tag{10}$$

Sub-index *i* accounts for the *i*-segment.

The battery capacity depends on the discharge rate [28]:

$$C_i^{bat} = f_C C_n^{bat} = 0.957 \frac{\left(C_n^{bat}\right)^{1.0148}}{\left(I_i\right)^{0.0148}} \tag{11}$$

Combining equations 10 and 11:

$$DOD_i^{bat} = 1.045 \eta_g t_i \left(\frac{I_i}{C_n^{bat}} \right)^{1.0148} \tag{12}$$

We realize that the partial DOD for a specific route segment depends on the discharge current and time.

If we use the supercapacitor for energy supply:

$$DOD_i^{sc} = \frac{2\xi_i}{V_{op} Q} \tag{13}$$

The supercapacitor charge depends on its capacity and resistance as in Equation 14:

$$Q = \begin{vmatrix} Q_o e^{-t/\tau} \\ Q_o \left(1 - e^{-t/\tau}\right) \end{vmatrix} \tag{14}$$

The upper expression in Equation 14 accounts for discharging, and the lower for charging. The time constant, τ, is the product of capacity, C^{sc}, and resistance, R;

$$\tau = RC^{sc} \tag{15}.$$

Replacing upper section of equation 14 in equation 13:

$$DOD_i^{sc} = \frac{2\xi_i}{V_{op} Q_o e^{-t/\tau}} \tag{16}$$

We observe that the supercapacitor charge and discharge process are opposite, showing the same pattern provided the time constant does not change; therefore, since the supercapacitor recharges from the battery, it seems that it makes no difference to use the battery or the supercapacitor for a given process since the energy we obtain from the supercapacitor must be replaced by the battery at the same rate, given that the charging and discharging process of the supercapacitor is identical in each case, regarding the evolution of the extracted or supplied intensity. In such a case, the battery DOD associated to the supercapacitor charge is:

$$DOD_i^{bat-sc} = \frac{2\xi_i}{V_{op} Q_o \left(1 - e^{-t/\tau}\right)} \tag{17}$$

Nevertheless, if the supercapacitor charging time extends because the time interval between consecutive uses delays, the supercapacitor charge and discharge process is not identical, influencing the battery discharge process when charging the supercapacitor. The supercapacitor charging delays by modifying the resistance since the capacity remains constant.

Considering a higher resistance for the supercapacitor, the battery discharge ratio is:

$$\frac{I_x}{I_o}=\frac{1-e^{-t/\tau_x}}{1-e^{-t/\tau_o}} \tag{18}$$

Sub-indexes o and x account for the initial and extended time discharge. Now, replacing in equation 12:

$$f_{DOD}^{bat}=\frac{DOD_{i,x}^{bat}}{DOD_{i,o}^{bat}}=\left(\frac{I_x}{I_o}\right)^{1.0148}=\left(\frac{1-e^{-t/\tau_x}}{1-e^{-t/\tau_o}}\right)^{1.0148}=\left(\frac{1-e^{-t/R_xC}}{1-e^{-t/R_oC}}\right)^{1.0148} \tag{19}$$

The coefficient f_{DOD}^{bat} represents the change in the battery DOD when modifying the supercapacitor resistance. We realize that the coefficient lowers when $R_x>R_o$ and vice versa.

Considering the electric vehicle driving range as the segment summation of the repetitive process of the protocol cycle:

$$DR=N\eta_t\left(\sum_{i=1}^{n}DOD_i^{bat}+\sum_{j=1}^{m}DOD_j^{sc}\right)=N\eta_t\left[\sum_{i=1}^{n}1.045\eta_g t_i\left(\frac{I_i}{C_n^{bat}}\right)^{1.0148}+\frac{2}{V_{op}Q_o}\sum_{j=1}^{m}\frac{\xi_j}{\left(1-e^{-t_j/\tau_j}\right)}\right] \tag{20}$$

N represents the number of protocol cycle repetitions.

Equation 20 determines the electric vehicle driving range as a function of the supercapacitor and battery capacity, the operating voltage, the energy demand, the discharge rate, and the driving time. Besides, energy transmission efficiency, power generation performance, and supercapacitor resistance influence the driving range.

SYSTEM DESIGN AND OPERATION

The hybrid power system is connected in parallel to supply energy to the electric motor indistinctly. Figure 1 shows the schematic diagram of the electric circuit.

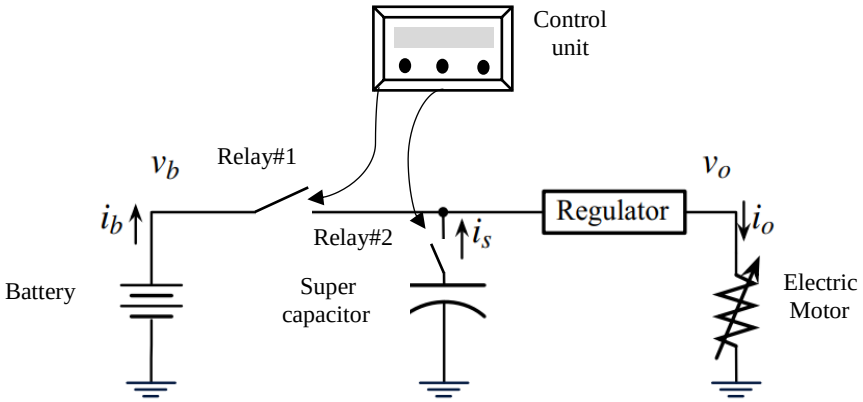

Figure 1. Schematic diagram of the electric circuit for the hybrid power sourceThe electric circuit equips two relays commanded by a control unit, which opens and closes the relays depending on the operating conditions. If power demand exceeds the setup threshold, the battery relay opens, and the supercapacitor relay closes. The electric motor runs on the supercapacitor for this configuration; if power demand falls below the threshold, the control unit opens the supercapacitor relay and closes the battery one. If the power demand exceeds the expected upper limit, the control unit closes both relays,

and the two power sources supply energy to the electric motor; however, this situation is purely incidental and only stands for a short time.

The hybrid supercapacitor/battery configuration is characterized by a higher power density inherent to the supercapacitor and allows a significant increase in the amount of discharge current. This increase effectively contributes to mitigating the adverse effects associated with higher discharge intensity, resulting in an overall improvement in system performance.

In non-continuous charging conditions, the supercapacitor assumes an additional function as a filter, reducing the maximum voltages experienced by the battery. This behavior is essential to maintain system stability, integrity, and battery life. It demonstrates the added value of integrating both components in a hybrid design.

The performance of this type of energy storage, characterized and evaluated under pulsed charging currents, has been subject to exhaustive comparison with systems that exclusively use batteries. These benchmarks provide a complete understanding of the advantages and challenges associated with hybrid energy storage systems adoption in various practical applications [29].

The selected electric vehicle prototype for evaluation is a Sport Utility Vehicle (SUV) model Toyota RAV4 whose characteristics are listed in Table 1 [30].

We should mention that we use the prototype as a reference since this model is not a full electric vehicle; therefore, we apply some specific characteristics for our study like size, aerodynamic coefficient and weight.

For the operating voltage we selected 400 V, which is a current value for electric vehicle's motor, and for the battery energy capacity 80 kWh corresponding to a vehicle mass of 2500 kg. These values match the standard reference data from the literature [31-].

.

Parameter	Value	Unity
Weight	2710	kg
Front side area	3.135	m^2
Aerodynamic coefficient	0.32	---

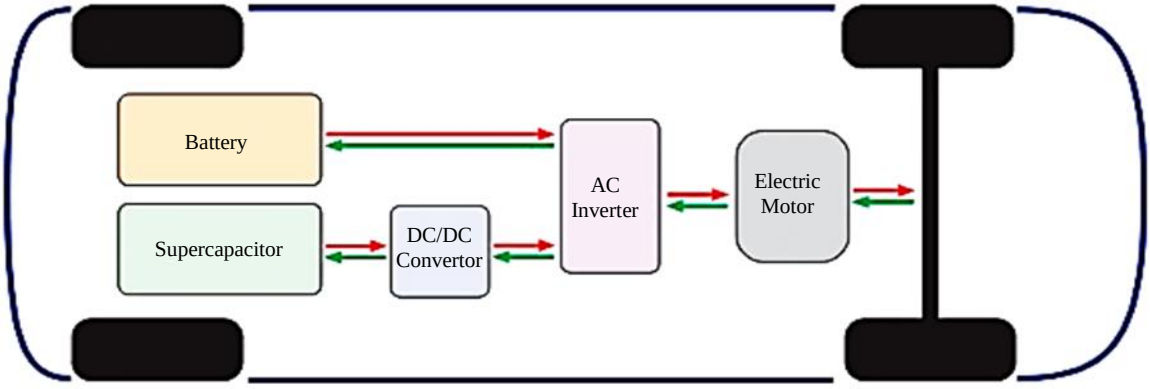

Figure 2. Schematic view of the system layout.

The electric motor operates at alternate current because this is the most frequent option selected by the electric vehicle manufacturers; therefore, a DC/AC inverter should be included in the system layout. Furthermore, since the supercapacitor supplies energy at different voltage than battery and electric motor, a DC/DC converter in intercalated in the electric wiring from supercapacitor to the inverter. Figure 2 shows the schematic view of the system layout.

For the supercapacitor, based on previous studies applied to electric vehicles [31-], we select a 25-unit pack of 5 F each, operating at a voltage of 2.5 volts per cell with a unit weight of 0.5 kg.

CONTROL PROCESS

The present study intends to apply to any electric vehicle and driving pattern; therefore, we design a control process to determine the supercapacitor and battery energy capacity that fits the daily route under current driving conditions. To this goal, we develop a control program that evaluates the supercapacitor and battery capacity and determines if the selected value fulfills energy requirements.

The program sets up a specific value for the supercapacitor and battery capacity and runs the WLTP protocol for this hybrid power system using the vehicle and road characteristics; if the supercapacitor state of charge, after any intermediate step supplying power to the electric motor, remains positive, the selected value is accepted and recorded in the database, if not, the program assigns a new capacity value for the supercapacitor, and the program restarts.

A similar process runs for the battery with the only difference that the battery checking is at the end of the WLTP cycle; if the state of charge remains positive, the selected value is accepted and recorded in the database; otherwise, the program assigns a new capacity value for the battery and the program restarts. Figure 3 shows the flowchart of the control process.

SIMULATION

The simulation runs on a MATLAB program with vehicle characteristics, speed, and operating time as input data. The power demand threshold is set up before launching the program. The flowchart of Figure 4 shows the protocol structure.

The control unit receives information about the power demand corresponding to the driving conditions and compares the value with the setup threshold. If the power demand is above the threshold, the control unit closes relay #2 and activates the supercapacitor, which starts supplying energy to the electric motor; if not, it commutes the power supply from the supercapacitor to the battery opening relay #2 and closing relay #1.

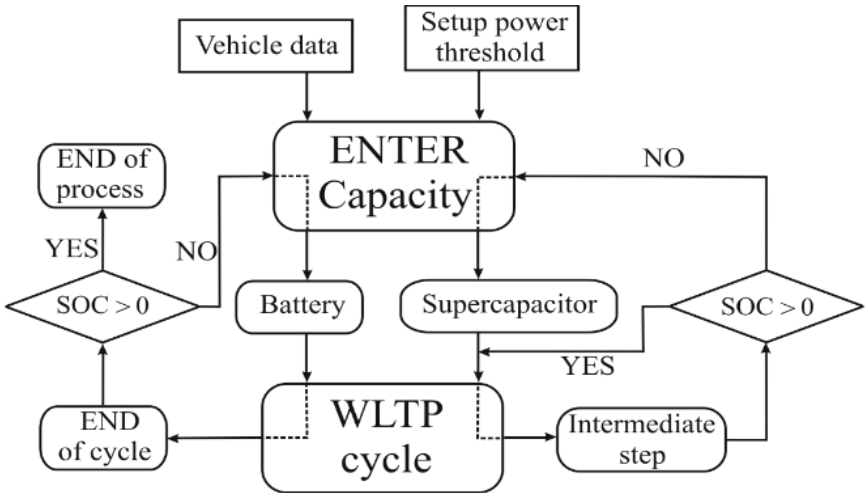

Figure 3. Flowchart of the control process

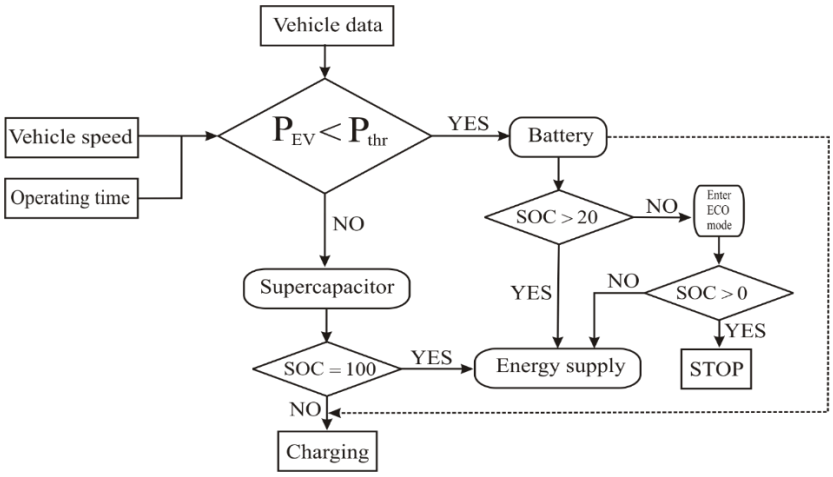

Figure 4. Flowchart of the simulation protocol.

During this process, the control unit monitors the state of charge of the battery and supercapacitor; if the supercapacitor is charged, the battery to supercapacitor circuit opens, and the supercapacitor charge stops; otherwise, the battery charges the supercapacitor to maintain it at full state of charge. If the battery reaches the 20% state of charge, the control unit switches the power supply to ECO mode, reducing the acceleration and limiting the vehicle speed to preserve energy; when the battery reaches the null state of charge, the vehicle stops.

The simulation uses the WLTP protocol as a reference to reproduce driving conditions; to this goal, we parametrize the WLTP protocol, so the program collects data, vehicle speed, and time from driving conditions at every moment. With these data, the program calculates the acceleration and average speed to determine power demand, which is the reference input for the control protocol. Figure 5 shows the vehicle speed and power demand according to the WLTP protocol for our prototype. We apply Equations 3 to 5 for the power acceleration and average vehicle speed determination.

To start the simulation we introduce the driving pattern, ECO, normal or sport; the program automatically sets up the reference value for the acceleration from which it determines the power threshold. Figure 6 shows the hybrid power source performance for specific power demand threshold.

We realize that the supercapacitor is inactive while the power demand remains below the threshold (red line in the upper section of Figure 6), turning on as soon as the power demand crosses the threshold line. When the control unit switches back the power supply to the battery, the supercapacitor starts charging from the battery until it reaches the 100% state of charge (horizontal blue line in the lower section of Figure 6).

We call the reader's attention to the supercapacitor energy evolution curve, which never reaches zero value, which shows a good supercapacitor size design. If the supercapacitor reaches zero value, the control unit claims for energy supply from the battery, which forces it to discharge at an unexpectedly high rate; this reduces the driving range, generates premature degradation, and reduces battery lifespan.

Regarding the battery behavior (Figure 7), we realize the battery discharges continuously, powering the electric vehicle or charging the supercapacitor. As in the case of the supercapacitor, the battery never reaches the null state of charge, proof that the battery size is correct. Figure 7 splits into drawing lines and a bar graph to facilitate the comprehension of the battery state of charge evolution.

In practice, the control unit only shows the current battery state of charge on the dashboard, similar to the remaining fuel level in conventional cars. The control unit also indicates the final battery state of charge at the end of the daily route. Upon request, the control unit shows the supercapacitor's remaining charge. Figure 8 shows the dashboard information.

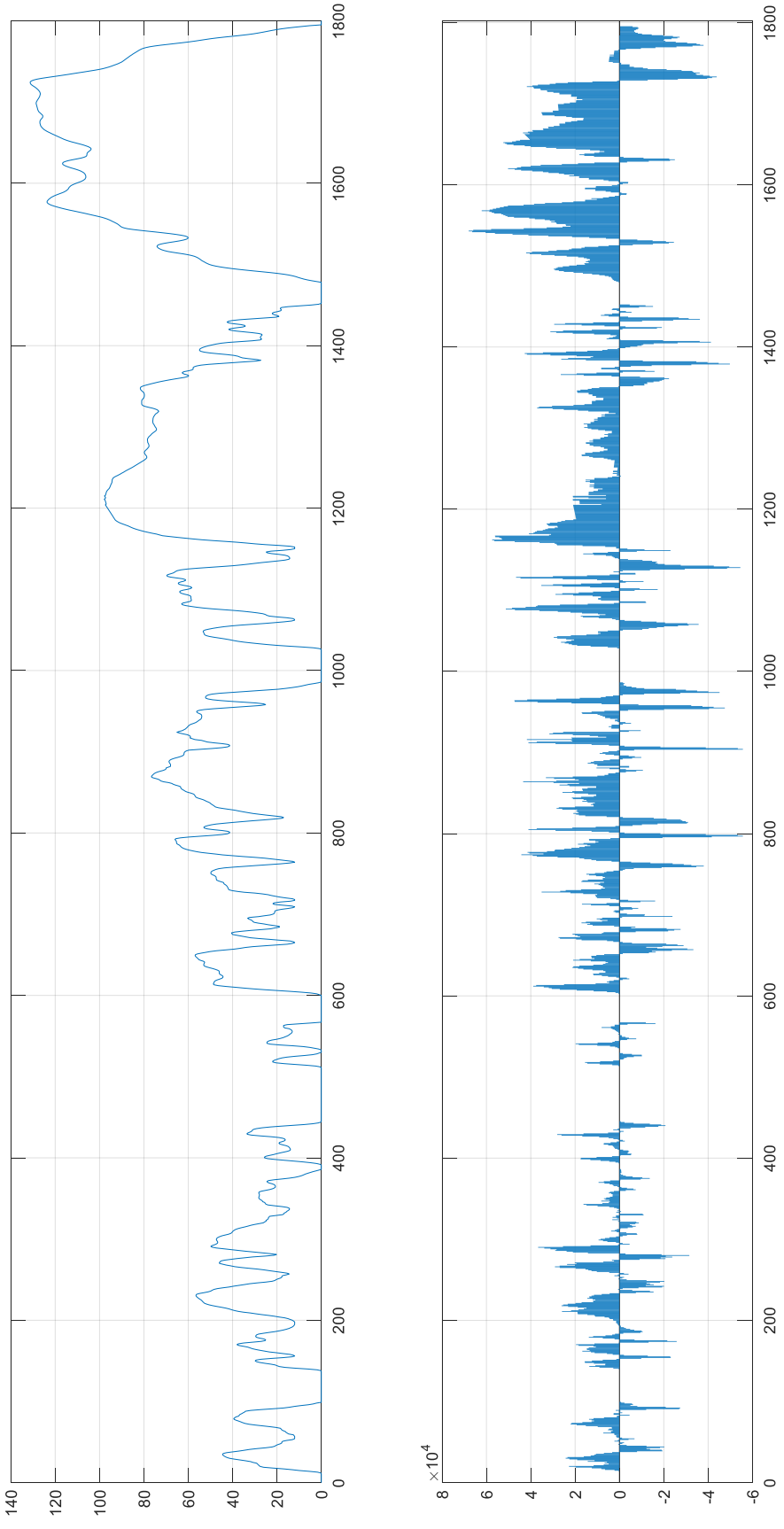

Figure 5. Evolution of prototype vehicle speed and power demand for WLTP protocol (ECO driving mode)

s

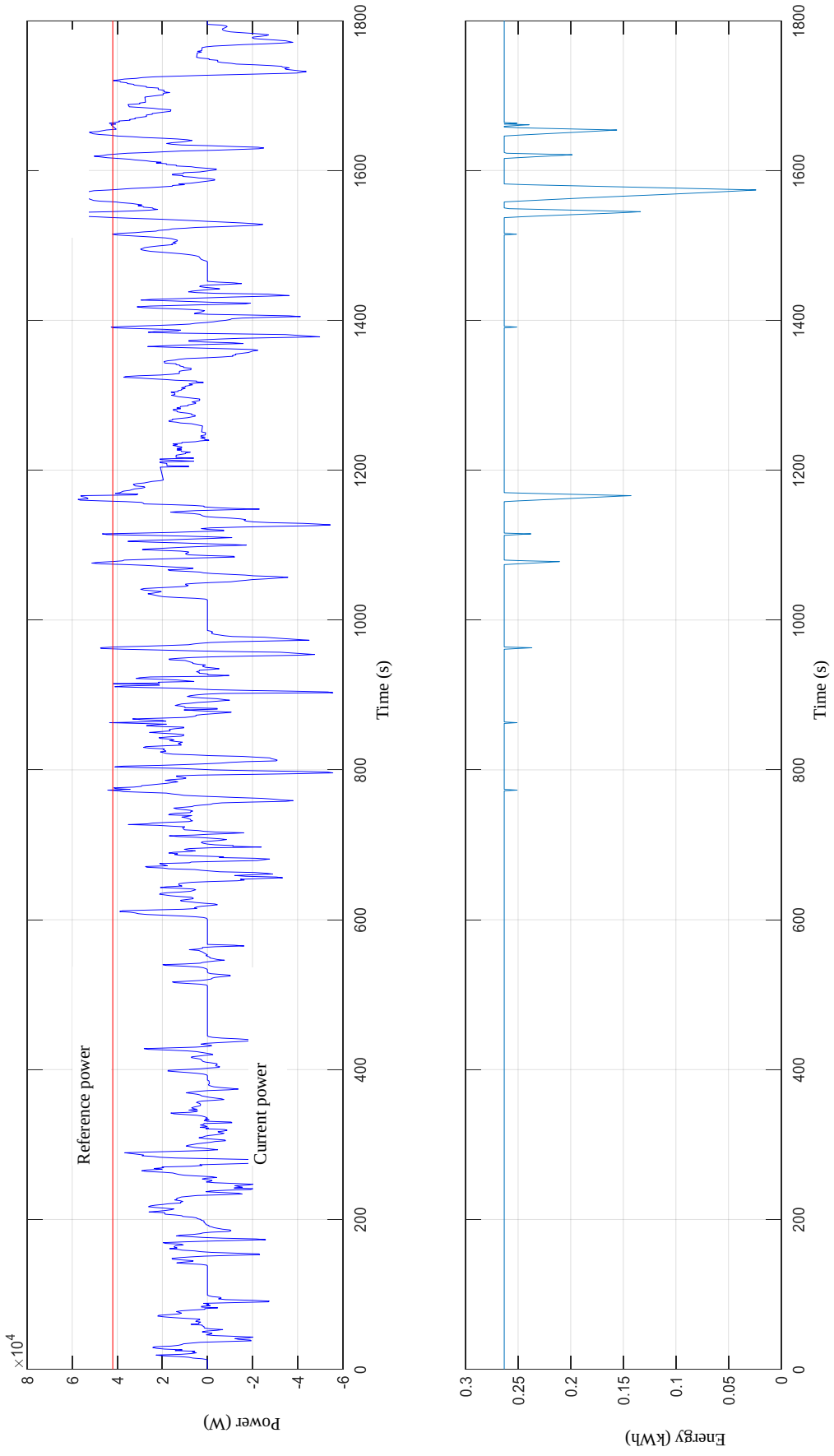

Figure 6. Evolution of prototype power demand (up) and supercapacitor charge (down) for specific driving conditions (ECO driving mode)

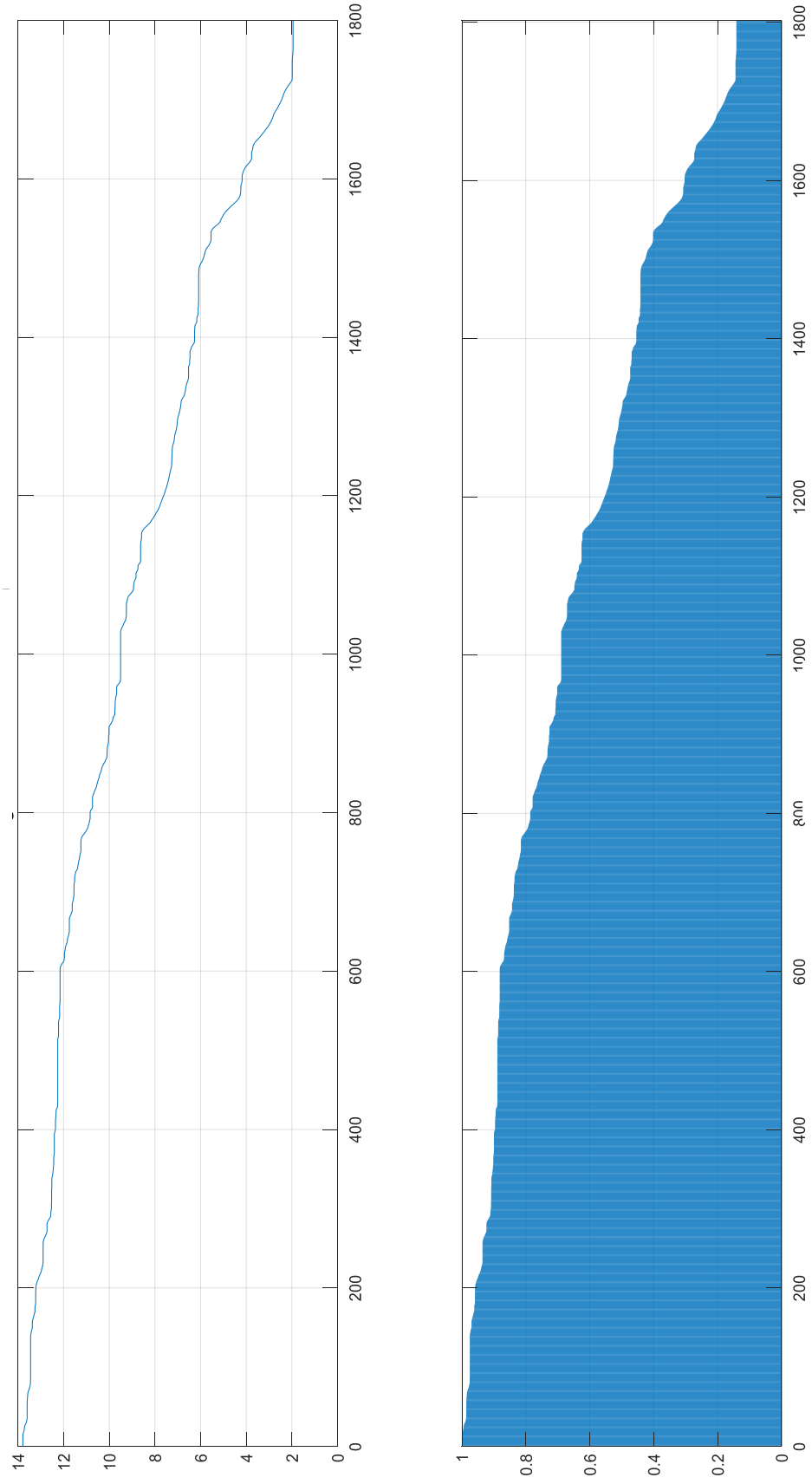

Figure 7. Evolution of battery state of charge evolution for specific driving conditions (ECO driving mode)

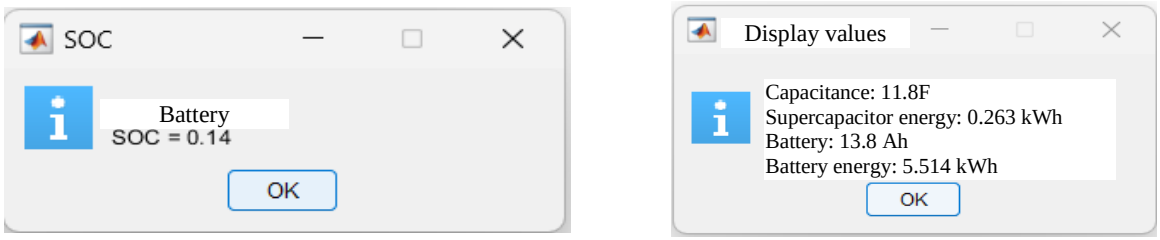

Figure 8. Dashboard information of battery and supercapacitor state of charge at the end of daily route (ECO driving mode)

Table 2. Driving pattern characteristics.

Driving pattern	Acceleration (m/s^2)	Power threshold (kW)
ECO	1.00	42
Normal	2.25	84
Sport	3.40	120

We repeat the simulation for normal and sport driving mode. Acceleration and power threshold for the three driving patterns are listed in Table 2.

Figures 9 to 14 show the simulations results for normal and sport driving mode.

ANALYSIS OF RESULTS

The simulation results agree with the expected data from theoretical development. Indeed, as we move from ECO to sport driving mode, the power demand and the power threshold increase in close agreement with the acceleration value, leading to a higher battery and supercapacitor energy capacity size.

When adjusting the reference power, we observe a variation in the nominal value of the capacity and energy of both the supercapacitor and the battery. The lower the threshold value, the more energy is required from the supercapacitor and less from the battery; if the threshold value increases, the effect is the opposite.

Since each driving mode and reference power setting produces different results in terms of ratings, we also note that there is a maximum reference power for which the battery and supercapacitor power may or may not meet the duty cycle driving. When the configuration is extreme, the supercapacitor and battery power may not be enough to fulfill their function.

We design the battery and supercapacitor to match the protocol driving cycle, driving mode, and power reference. Although some configurations fulfill the protocol driving cycle, we should design the vehicle performance for a higher driving range. In this sense, the battery capacity becomes critical since the supercapacitor uses the same battery to recharge, thus eliminating the need to recalculate its capacity. Considering that the WLTP cycle has a distance of 23.2781 km, to provide the vehicle with a range of 300 km, the value of the battery capacity must be multiplied by 14 to satisfy the requirement imposed by the WLTP cycle.

On the other hand, the results show that the simulation is capable of establishing the capacity and energy values necessary to operate a vehicle with a battery/supercapacitor hybrid power system under the conditions established by the WLTP standard protocol, adjusting said values to the established driving, which means a relevant achievement in the development of prediction and control systems for

electric vehicles.

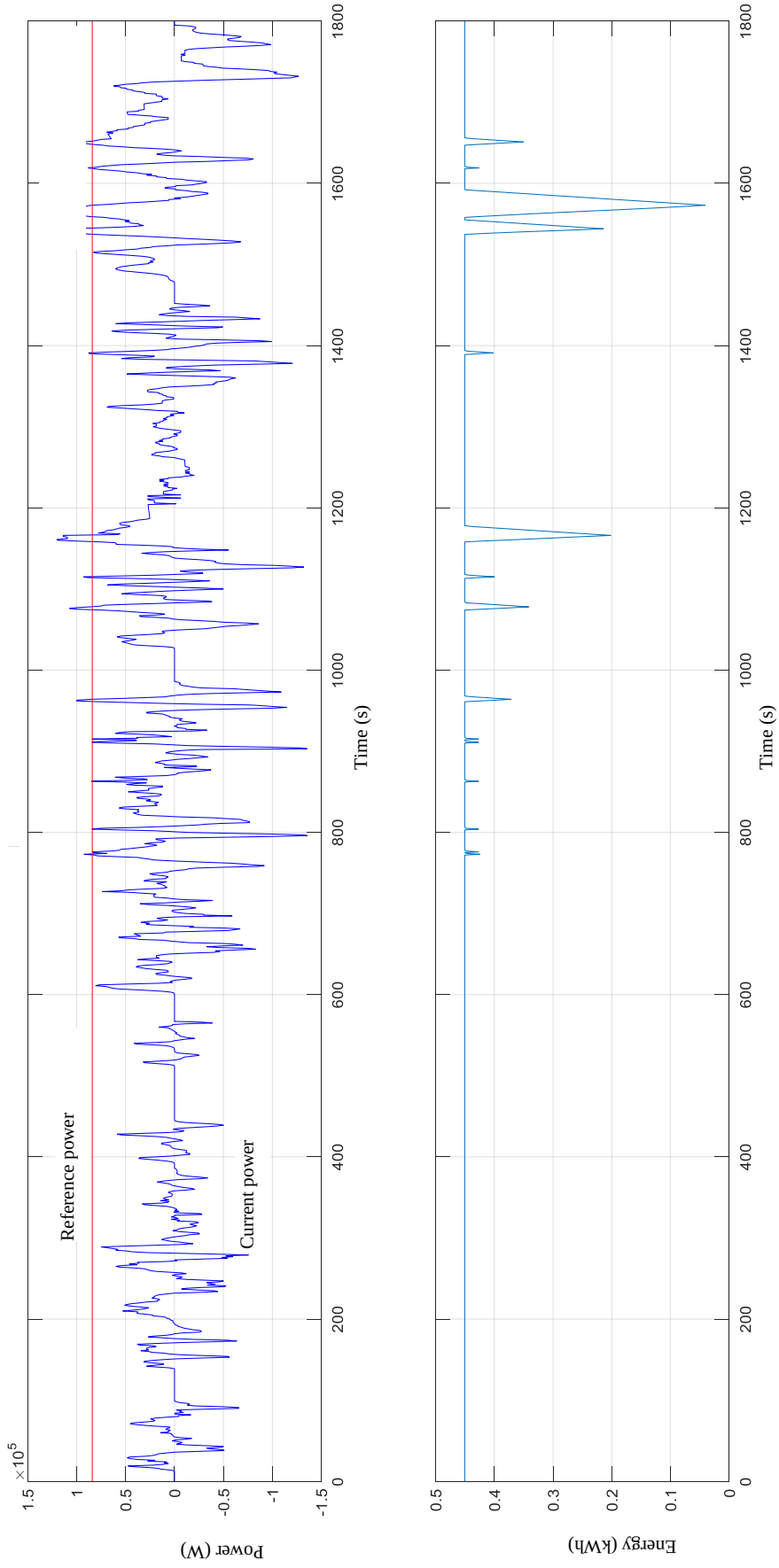

Figure 9. Evolution of prototype power demand (up) and supercapacitor charge (down) for specific driving conditions (normal driving mode)

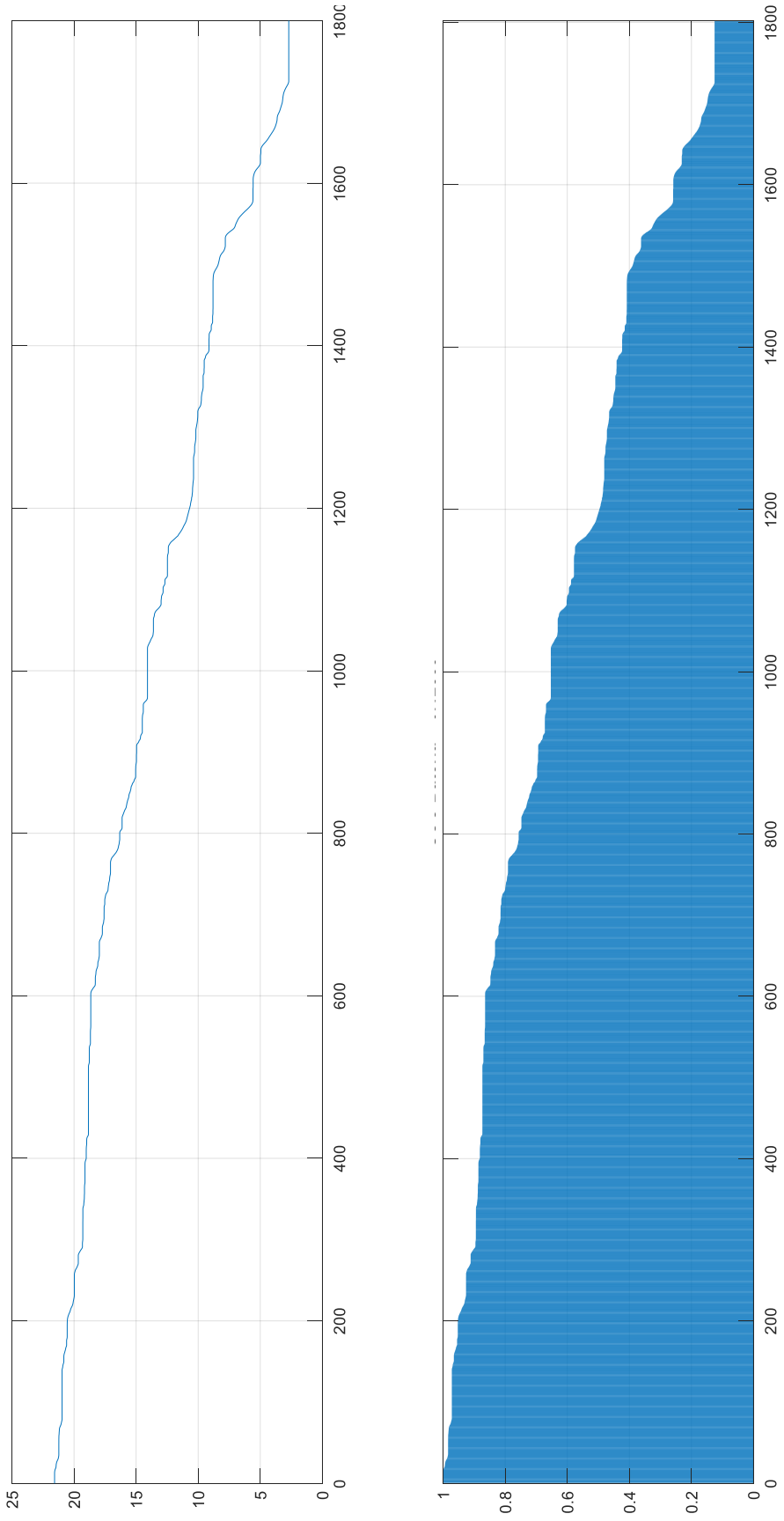

Figure 10. Evolution of battery state of charge evolution for specific driving conditions (normal driving mode)

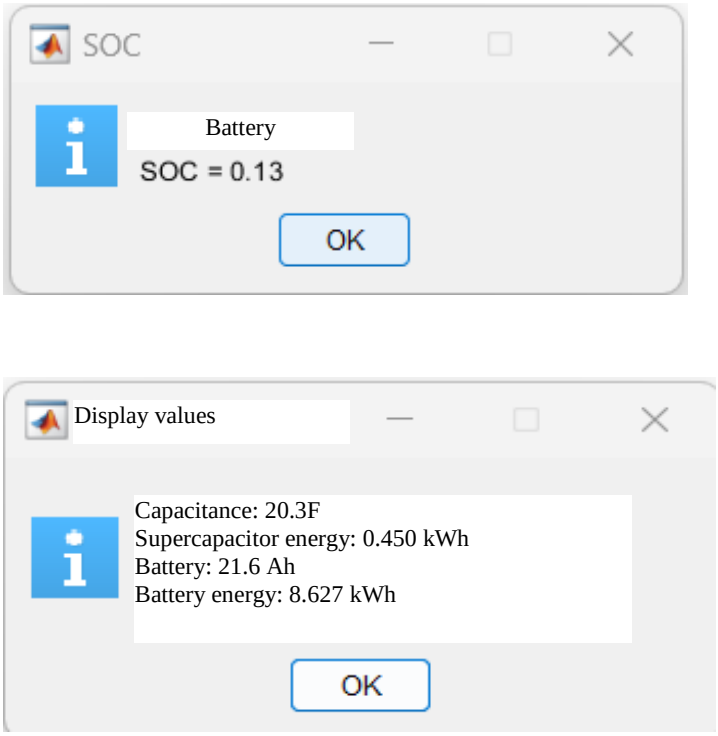

Figure 11. Dashboard information of battery and supercapacitor state of charge at the end of daily route (normal driving mode)

The simulation program calculates the new values of battery and supercapacitor energy capacity as a function of the driving conditions and driving pattern so that the state of charge of the supercapacitor and the battery are always positive or identically zero. The simulation results shown in Figures 6, 7, 9, 10, 12, and 13 for the ECO, normal, and sport driving mode verify this statement.

CONCLUSIONS

The hybrid lithium battery and supercapacitor combination offers a unique synergy that improves system responsiveness, reduces operational stress, and promotes greater energy efficiency.

This approach represents a significant energy management advance and has potential applications in many fields, from electric vehicles to energy storage systems.

The hybrid system of supercapacitor and lithium battery has better performance than a system with a single energy source (battery) due to the fact of transferring high power demand processes, which require very high discharges, from the battery to the supercapacitor, which reduces premature degradation and aging of the battery, lengthening its average life and increasing the reliability of its response.

The hybrid supercapacitor/lithium battery system guarantees less battery wear and power system efficiency improvement by operating each energy subsystem, battery, or supercapacitor in the range of most suitable power. The limitation in battery high power draining increases the battery and supercapacitor lifespan.

The correct sizing of the battery and supercapacitor from the simulation process guarantees continuous vehicle operation for specific driving conditions, providing a practical tool for electric

vehicle manufacturers and designers.

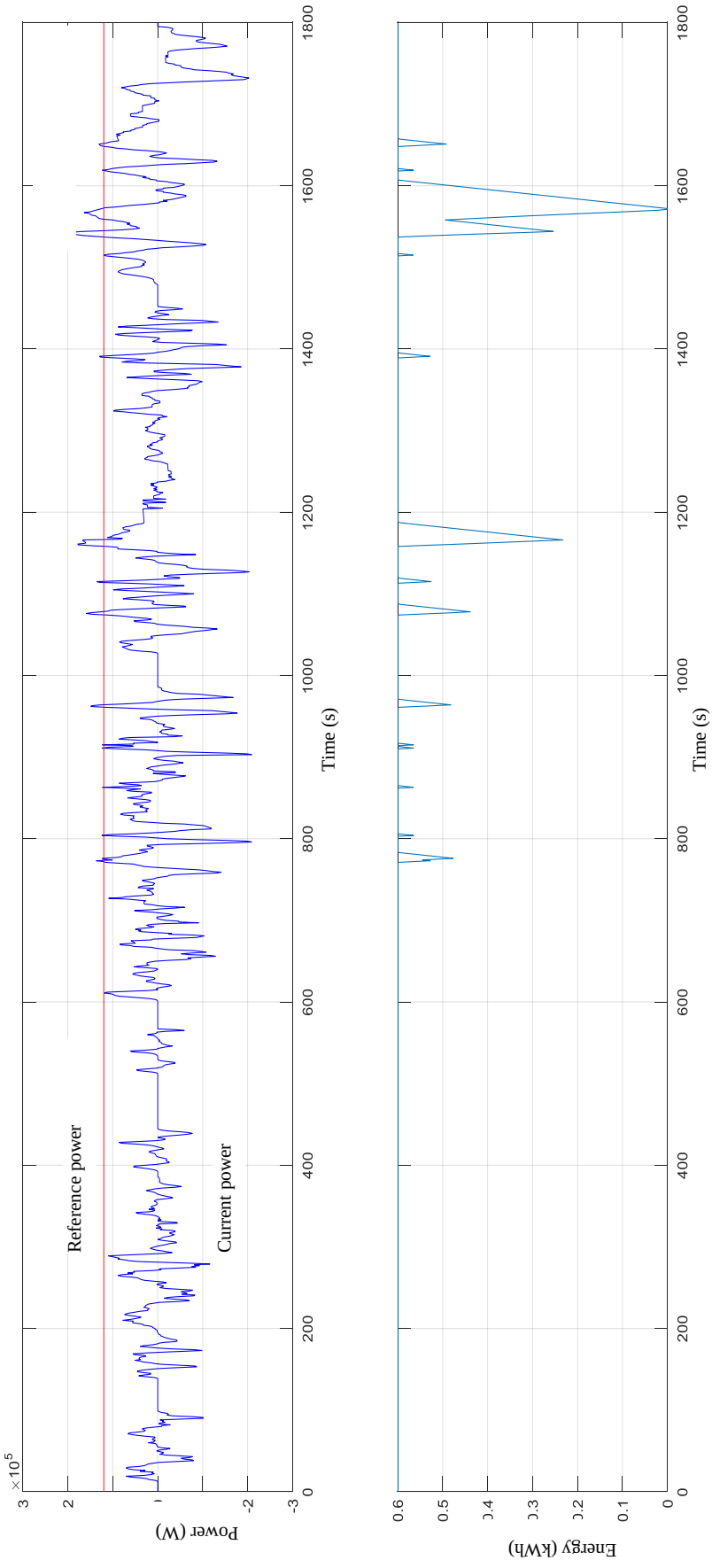

Figure 12. Evolution of prototype power demand (up) and supercapacitor charge (down) for specific driving conditions (sport driving mode)

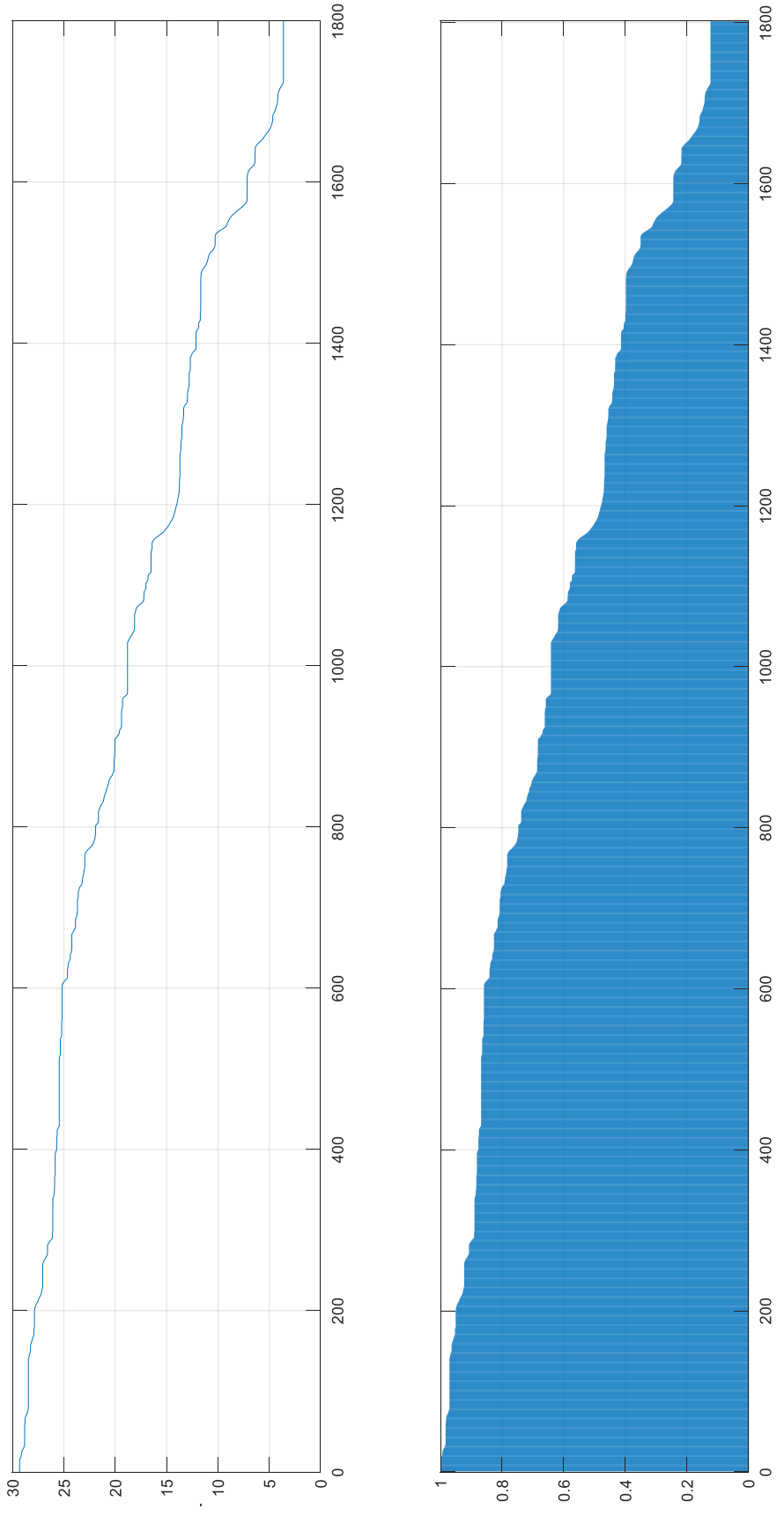

Figure 13. Evolution of battery state of charge evolution for specific driving conditions (normal driving mode)

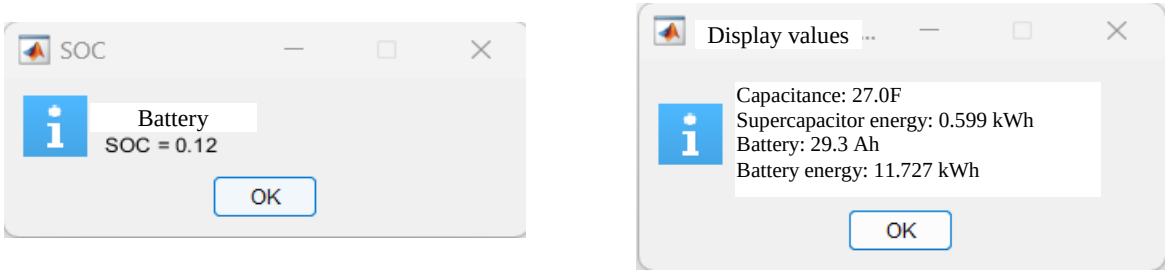

Figure 14. Dashboard information of battery and supercapacitor state of charge at the end of daily route (sport driving mode)

REFERENCES

1. Sioshansi, R., & Denholm, P. (2009). Emissions impacts and benefits of plug-in hybrid electric vehicles and vehicle-to-grid services. *Environmental Science & Technology*, *43*(4), 1199–1204.
2. Casals, L. C., Martinez-Laserna, E., García, B. A., & Nieto, N. (2016). Sustainability analysis of the electric vehicle use in Europe for CO2 emissions reduction. Journal of Cleaner Production, 127, 425–437.
3. Peters, G. P., Marland, G., Le Quéré, C., Boden, T., Canadell, J. G., & Raupach, M. R. (2012). Rapid growth in CO2 emissions after the 2008–2009 global financial crisis. Nature Climate Change, 2(1), 2–4.
4. Zhang, X., Karplus, V. J., Qi, T., Zhang, D., & He, J. (2016). Carbon emissions in China: How far can new efforts bend the curve?. Energy Economics, 54, 388–395.
5. Matthews, H. D., Gillett, N. P., Stott, P. A., & Zickfeld, K. (2009). The proportionality of global warming to cumulative carbon emissions. Nature, 459(7248), 829–832.
6. Solomon, S., Plattner, G. K., Knutti, R., & Friedlingstein, P. (2009). Irreversible climate change due to carbon dioxide emissions. Proceedings of the National Academy Of Sciences, 106(6), 1704–1709.
7. Armenta-Déu, C., & Cattin, E. (2021). Real driving range in electric vehicles: Influence on fuel consumption and carbon emissions. World Electric Vehicle Journal, 12(4), 166.
8. Laurikko, J., Granström, R., & Haakana, A. (2012). Assessing range and performance of electric vehicles in Nordic driving conditions–Project" RekkEVidde". World Electric Vehicle Journal, 5(1), 45–50.
9. Helmbrecht, M., Olaverri-Monreal, C., Bengler, K., Vilimek, R., & Keinath, A. (2014). How electric vehicles affect driving behavioral patterns. IEEE Intelligent Transportation Systems Magazine, 6(3), 22–32.
10. Van Haaren, R. (2011). Assessment of electric cars' range requirements and usage patterns based on driving behavior recorded in the National Household Travel Survey of 2009. Earth and Environmental Engineering Department, Columbia University, Fu Foundation School of Engineering and Applied Science, New York, 51, 53.
11. Bingham, C., Walsh, C., & Carroll, S. (2012). Impact of driving characteristics on electric vehicle energy consumption and range. IET Intelligent Transport Systems, 6(1), 29–35.
12. Wikipedia. (2025). New European Driving Cycle (NEDC). [Online]. Wikipedia. Available from: https://en.wikipedia.org/wiki/New_European_Driving_Cycle.
13. Wikipedia. (2025). Worldwide Harmonised Light Vehicles Test Procedure. [Online]. Wikipedia. Available from: https://en.wikipedia.org/wiki/Worldwide_Harmonised_Light_Vehicles_Test_Procedure.
14. Wikipedia. (2025). FTP-75 (EPA Federal Test Procedure). [Online]. Wikipedia. Available from: https://en.wikipedia.org/wiki/FTP-75.
15. Japan Inspection Organization. (2022). Japanese JC08 Emission Test Cycle. [online] Available from: https://japaninspection.org/japanese-jc08-emission-test-cycle/
16. Alphabet. (2025). WLTP Explained - What Is It & How It Affects Businesses. [Online] Available

from: www.alphabet.com/en-gb/wltp.
17. Xun, Q., Liu, Y., & Holmberg, E. (2018, June). A comparative study of fuel cell electric vehicles hybridization with battery or supercapacitor. In 2018 International Symposium on Power Electronics, Electrical Drives, Automation and Motion (SPEEDAM) (pp. 389–394). IEEE.
18. Khaligh, A., & Li, Z. (2010). Battery, ultracapacitor, fuel cell, and hybrid energy storage systems for electric, hybrid electric, fuel cell, and plug-in hybrid electric vehicles: State of the art. IEEE Transactions on Vehicular Technology, 59(6), 2806–2814.
19. Chau, K. T., & Wong, Y. S. (2001). Hybridization of energy sources in electric vehicles. Energy Conversion and Management, 42(9), 1059–1069.
20. EV Database. Useable battery capacity of full electric vehicles cheatsheet. [Online]. EV Database. https://ev-database.org/cheatsheet/useable-battery-capacity-electric-car [Accessed online: 17/11/2023].
21. Das, H. S., Tan, C. W., & Yatim, A. H. M. (2017). Fuel cell hybrid electric vehicles: A review on power conditioning units and topologies. Renewable and Sustainable Energy Reviews, 76, 268–291.
22. Changizian, S., Ahmadi, P., Raeesi, M., & Javani, N. (2020). Performance optimization of hybrid hydrogen fuel cell-electric vehicles in real driving cycles. International Journal of Hydrogen Energy, 45(60), 35180–35197.
23. Fernández, R. Á., Cilleruelo, F. B., & Martínez, I. V. (2016). A new approach to battery powered electric vehicles: A hydrogen fuel-cell-based range extender system. International Journal of Hydrogen Energy, 41(8), 4808–4819.
24. Armenta-Déu, C. (2024) Improving Sustainability in Urban and Road Transportation: Control Device for Dual Battery Block and Fuel Cell Hybrid Power System for Electric Vehicles, Sustainability, 16(5), 2110 https://www.mdpi.com/2071–1050/16/5/2110 https://www.mdpi.com/2071–1050/16/5/2110/pdf
25. Armenta-Déu, C., Cortés, H. (2023) Real consumption protocol for driving range determination in EV: application to urban routes. International Journal of Vehicle Systems Modelling and Testing, Volume 17, Nos 3/4, pages 244–266 https://doi.org/10.1504/IJVSMT.2023.135447
26. Kouchachvili, L., Yaïci, W., Entchev, E. (2018) Hybrid battery/supercapacitor energy storage system for the electric vehicles, J Power Sources, vol. 374, pp. 237–248. https://doi.org/10.1016/J.JPOWSOUR.2017.11.040
27. Shchur, I., & Biletskyi, Y. (2018, April). Battery Currents Limitation in Passivity Based Controlled Battery/Supercapacitor Hybrid Energy Storage System. In 2018 IEEE 38th International Conference on Electronics and Nanotechnology (ELNANO) (pp. 504–510). IEEE.
28. Armenta-Déu, C., Carriquiry, J.P., Guzmán, S. (2019) Capacity correction factor for Li-ion batteries: influence of the discharge rate. Journal of Energy Storage, Volume 25, October 2019, 100839 doi: https://doi.org/10.1016/j.est.2019.100839.
29. Xia, S., Chen, L. Theoretical and experimental investigation of optimal capacitor charging process in RC circuit. https://doi.org/10.1140/epjp/i2017–11507–8
30. Toyota. (2025). Toyota RAV4 features. [Online] Available from: https://www.toyota.com/rav4/rav4-features/
31. Thangavel, S., Mohanraj, D., Girijaprasanna, T., Raju, S., Dhanamjayulu, C., Muyeen, S.M. (2023) A Comprehensive Review on Electric Vehicle: Battery Management System, Charging Station, Traction Motors, IEEE Access, vol. 11. Institute of Electrical and Electronics Engineers Inc., pp. 20994–21019. https://doi.org/10.1109/ACCESS.2023.3250221

